Available online at www.sciencedirect.com

ScienceDirect

Reactive & Functional Polymers 67 (2007) 1398–1407

REACTIVE & FUNCTIONAL POLYMERS

www.elsevier.com/locate/react

# Thermal modulation of intracellular drug distribution using thermoresponsive polymeric micelles

M. Nakayama [a], J.E. Chung [a], T. Miyazaki [b], M. Yokoyama [a,c], K. Sakai [b], T. Okano [a,*]

[a] *Institute of Advanced Biomedical Engineering and Science, Tokyo Women's Medical University, Kawada-cho 8-1, Shinjuku-ku, Tokyo 162-8666, Japan*

[b] *Department of Applied Chemistry, Waseda University, 3-4-1, Ohkubo, Shinjuku-ku, Tokyo 169-8555, Japan*

[c] *Kanagawa Academy of Science and Technology, Yokoyama "Nano-medical polymers" project, KSP East 404, Sakado 3-2-1, Takatsu-ku, Kawasaki-shi, Kanagawa 213-0012, Japan*

Received 12 June 2007; received in revised form 25 July 2007; accepted 26 July 2007
Available online 9 August 2007

Dedicated to Professor Teiji Tsuruta on the occasion of his 88th birthday (Beiju).

**Abstract**

Intracellular distribution of free doxorubicin (DOX) or DOX-loaded in polymeric micelles with thermoresponsive outer shells of poly(*N*-isopropylacrylamide) or its copolymers in cultured human breast cancer cells (MCF-7) were investigated by fluorescence and confocal laser scanning microscopy. Free DOX accumulated rapidly and selectively in cell nuclei, independent of temperature changes. In contrast to free drugs, the intracellular distribution of DOX-loaded in the thermoresponsive polymeric micelles was significantly affected by temperature changes across lower critical solution temperature (LCST) of the micelles. Above the micelle LCST, DOX delivered by the micelles was localized uniformly inside of MCF-7 cells. By contrast, the amount of DOX delivered to MCF-7 cells drastically decreased below the micelle LCST due to minimal interaction of the micelles with cell membrane surfaces. These results clearly showed that the mechanism of the intracellular drug localization was different between free drugs and DOX-loaded in the micelles. The thermoresponsive micelles aggressively interacted with the cells and carried DOX into the cells *via* triggered phase transition of the outer shells. In addition, much lower accumulation of free DOX was observed in the resistant cells compared to its parent sensitive MCF-7 due to the resistant mechanism. Of interest, DOX accumulation in the resistant cells was almost in the same level as with MCF-7 (sensitive) cells for the micelle system above the LCST.



*Keywords:* Poly(*N*-isopropylacrylamide); Thermoresponse; Polymeric micelles; Doxorubicin; Intracellular drug distribution

## 1. Introduction

Selective anti-cancer drug delivery to solid tumor tissues using drug carriers has been an extremely

* Corresponding author. Tel.: +81 3 3353 8112x30235; fax: +81 3 3359 6046.
*E-mail address:* tokano@abmes.twmu.ac.jp (T. Okano).

1381-5148/$ - see front matter © 2007 Elsevier Ltd. All rights reserved.
doi:10.1016/j.reactfunctpolym.2007.07.056

attractive application for cancer chemotherapy without severe toxic side effects. For this purpose, several types of drug carriers, such as water-soluble polymers [1,2], liposomes [3,4], and polymeric micelles [5], have been actively investigated.

Amphiphilic block copolymers form core-shell multi-molecular assemblies called polymeric micelles in aqueous media [6,7]. Highly hydrated outer shells of polymeric micelles provide their reliable structural stability in aqueous environments. Hydrophobic inner cores can incorporate a large amount of hydrophobic drug with maintaining their water-solubility due to the presence of the hydrophilic outer shells. Furthermore, nano-ordered diameter range of polymeric micelles (10–200 nm) can allow long circulation in the blood stream avoiding the body's defense systems (reticuloendotherial system, RES) and thus, utilize the enhanced permeability and retention (EPR) effect [8,9] at solid tumor sites for tumor targeting. We have previously reported that polymeric micelles composed of poly(ethylene oxide)-*b*-poly(L-asparate) block copolymers containing an anticancer drug, doxorubicin (DOX), selectively accumulated at solid tumor sites by the passive targeting mechanism, the EPR effect [10,11].

Recently, polymeric micelles with stimuli-responsive drug release mechanisms as a novel concept for anticancer drug delivery have been designed for applications in effective cancer chemotherapy [12–14]. The different drug release kinetics stimulated by physico-chemical signals (e.g., heat, pH, and ultrasound) may lead to maximal cytotoxic action at tumor sites, resulting in locoregional drug accumulation while reducing drug accumulation in normal tissues to inhibit undesirable side effects. These drug carrier systems combining two or more targeting methodologies is defined as multi-targeting systems. In order to accomplish these intelligent drug targeting systems, we have developed polymeric micelles possessing thermoresponsive outer shells [15–17]. Our strategy of cancer chemotherapy using the thermoresponsive polymeric micelles is as follows. Polymeric micelles with drugs circulate in the blood avoiding the RES uptake, and accumulate selectively at solid tumor tissues *via* the EPR-mediated targeting below the micelle LCST. And then the thermoresponsive outer shells of the micelles shrink and change into hydrophobic by local heating at the target sites upon the LCST. This alternation of micelle properties may induce selective drug actions at the heated target site. Simultaneously, this strategy can achieve temporal drug delivery control by local temperature increases.

Poly(*N*-isopropylacrylamide) (PIPAM) is well-known to undergo sharp coil-to-globule transitions at 32 °C in water [18]. This phase transition temperature is called a lower critical solution temperature (LCST). This polymer changes from water-soluble and hydrophilic state (coil) below its LCST to water-insoluble and hydrophobic state (globule: aggregation) above the LCST. Previously, we have already reported successful preparations of thermoresponsive polymeric micelles constructed with two block copolymers, PIPAM-*b*-poly(butyl methacrylate) [15] and PIPAM-*b*-poly(D,L-lactide) [16]. In our previous works, the DOX-loaded thermoresponsive micelles demonstrated successful controlled ON–OFF drug release and subsequent expression of *in vitro* cytotoxicity with applied temperature changes [15,17].

Here, we mainly focus on investigation of intracellular drug delivery and interactions of the thermoresponsive polymeric micelles into/with cultured human breast cancer (MCF-7) cells by fluorescence and laser scanning confocal microscopy in order to understand cytotoxic mechanisms modulated by temperature changes as well as to optimize drug carrier design for the multi-targeting systems.

## 2. Materials and methods

### 2.1. Materials

*N*-Isopropylacrylamide (IPAM) was kindly provided by Kohjin (Japan) and recrystallized from *n*-hexane. D,L-Lactide (LA, TCI, Japan) was purified by recrystallization from ethyl acetate. Butyl methacrylate (BMA, Tokyo Kasei Co. Ltd., Japan), *N*,*N*-dimethylacrylamide (DMAM, Wako Pure Chemicals, Japan) and 3-mercaptopropionic acid (Aldrich) were distilled under reduced pressure. Triethylamine and xylene were purchased from Wako Pure Chemicals and purified by standard methods. Benzoylperoxide (BPO, Kanto Chemical Co., Japan), *N*-ethylacetamide (TCI), *N*,*N*-dimethylacetamide (Wako Pure Chemicals), thionyl chloride (Wako Pure Chemicals), diethyl ether (Wako Pure Chemicals), 2-mercaptoethanol (Wako Pure Chemicals) and tin(II)2-ethylhexanoate (Wako Pure Chemicals) were used as received. Doxorubicin hydrochloride (DOX–HCl) was obtained from Mercian Co., Japan.

### 2.2. Synthesis of PIPAM-b-PBMA block copolymer

Hydroxyl-terminated poly(*N*-isopropylacrylamide) (PIPAM–OH) and carboxyl-terminated poly(butyl methacrylate) (PBMA–COOH) were prepared by telomerization using 2-mercaptoethanol (ME) and 3-mercaptopropionic acid as a chain transfer agent, respectively [15]. A molecular weight of the PIPAM–OH was determined by gel permeation chromatography (GPC; Tosoh, SC-8020, calibrated with polystyrene standards, elution rate: 1.0 ml/min) at 45 °C using DMF containing 10 mM LiCl as eluent. The terminal carboxyl functionality of the PBMA–COOH was determined by non-aqueous potentiometric titration using 0.01 N $CH_3ONa$ dissolved in a mixture of methanol and dioxane. Diblock copolymers of PIPAM and PBMA (PIPAM-*b*-PBMA) were obtained by reaction between a hydroxyl group of the PIPAM–OH and a carboxyl group of the PBMA–COOH by activation with thionyl chloride. The detailed synthetic and purification procedures of the block copolymers were reported in our previous paper [15].

### 2.3. Synthesis of P(IPAM–co–DMAM)-b-PLA block copolymer

Hydroxyl-terminated thermoresponsive polymers, poly(IPAM–*co*–DMAM) (P(IPAM–DMAM)–OH) was synthesized by radical copolymerization (20 mol% DMAM against total monomers) using ME [17]. Diblock copolymers were synthesized by ring opening polymerization of D,L-lactide (LA) from the hydroxyl end-group of the P(IPAM–DMAM)–OH as reported in our previous paper [17]. Briefly, the P(IPAM–DMAM)–OH polymers were dissolved in xylene. D,L-lactide and tin(II)2-ethylhexanoate as a catalysis were added to the polymer solution. Polymerization proceeded at 150 °C for 24 h under a nitrogen atmosphere. The obtained polymers were precipitated twice in an excess of diethyl ether, and then dried in vacuo. A molecular weight of the P(IPAM–DMAM)-*b*-PLA block copolymers was determined by GPC in the same conditions as for the PIPAM-*b*-PBMA. The composition of the block copolymers was determined with a $^1$H NMR spectrometer (400 MHz, Varian).

### 2.4. Preparation of DOX-loaded polymeric micelles

The formation of micelle structures and the DOX loading were simultaneously carried out by a dialysis method. The PIPAM-*b*-PBMA block copolymers (19 mg) and DOX–HCl (19 mg) were dissolved separately in 1.5 ml of *N*-ethylacetamide. The DOX solution was added to the polymer solution after addition of triethylamine (TEA) (6.0 μl, 1.3 molar equivalents versus DOX–HCl). The solution was dialyzed against distilled water at room temperature for 48 h (MWCO: 12,000–14,000, Spectra/Por 4, Spectrum Medical Industries). For the P(IPAM–DMAM)-*b*-PLA block copolymers, DOX–HCl (100 mg) was dissolved in 50 ml *N*,*N*-dimethylacetamide (DMAc) and added by TEA (1.5 molar equivalents versus DOX–HCl), followed by stirring for 10 min. P(IPAM–DMAM)-*b*-PLA block copolymers (100 mg) were dissolved in 50 ml DMAc. The DOX solution and the polymer solution were mixed at room temperature, followed by dialysis against distilled water using the dialysis membrane (MWCO: 12,000–14,000, Spectra/Por4) at room temperature. The obtained DOX-loaded polymeric micelles were ultrafiltrated using a filtration membrane of 200,000 molecular weight cut-off (ultrafilter Q2000, ADVANTEC MFS, INC.) at 4 °C to remove un-incorporated DOX. The UV absorbance at 485 nm was measured to estimate quantities of the incorporated DOX (V-530, Japan Spectroscopic Co., Japan) using molar extinction coefficient of DOX–HCl at 485 nm in distilled water.

### 2.5. Characterization of polymeric micelles

Optical transmittance of the 0.5 wt% polymeric micelle solutions (the PIPAM/PBMA micelles in water, and the P(IPAM–DMAM)/PLA micelles in phosphate buffer saline(PBS)) at various temperatures were measured at 600 nm with a UV–vis spectrometer. A sample cell was thermostated with a Peltier-effect cell holder (EHC-477, Japan Spectroscopic). Heating rate was 0.1 °C/min. The LCST of the micelle solutions was defined as the temperature inducing a 50% decrease in optical transmittance. Hydrodynamic diameters of the micelles were measured by dynamic light scattering (DLS) using a DLS-7000 instrument (Otsuka Electronics Co., Japan) equipped with He–Ne laser (633 nm).

### 2.6. Cell culture

Human breast cancer MCF-7 and its DOX-resistant (MCF-7/DOX) cell lines (kindly supplied by National Cancer Institute, USA) were grown as a monolayer in 75 $cm^2$ tissue culture flask containing

RPMI 1640 supplemented with 5% fetal bovine serum (FBS), 100 units/ml penicillin and 100 μg/ml streptomycin. All cell lines were cultured at 37 °C with 5% $CO_2$.

### 2.7. Intracellular distribution of DOX

Cells were plated at a density of $4 \times 10^4$ cells/well onto a glass slide with an aminoalkyl group-grafted surface (S-9215, Matsunami Glass, Japan) fitted with a culture vessel (flexiPERM, VIVASCIENCE, Germany). Cells were incubated in RPMI 1640 supplemented with 5% FBS, 100 units/ml penicillin and 100 μg/ml streptomycin. At 14 h after plating, cells were exposed to either free DOX (30 μg/ml) or the DOX-loaded micelles (incorporated DOX 30 μg/ml) in the cell culture medium and incubated at below (29 °C for the PIPAM/PBMA micelles, 37 °C for the P(IPAM–DMAM)/PLA micelles) or above (37 °C for the PIPAM/PBMA micelles, 42.5 °C or the P(IPAM–DMAM)/PLA micelles) the LCSTs of the micelles. After incubation for various periods, cells were gently rinsed with PBS to remove the micelles adhered to the cell membranes (non-incorporated micelles) at the temperature below the micelle LCST (25 °C). The cells on glass slides were fixed at room temperature with 4% paraformaldehyde for 30 min, and then washed with PBS containing 0.02% $NaN_3$. Nuclei of the treated cells were stained with Hoechst 33258 (10 μg/ml, Molecular Probes, USA) for 10 min at room temperature. Finally, the cells were washed three times with PBS containing 0.02% $NaN_3$ and observed by fluorescence microscopy (TE2000-U, Nikon, Japan) and laser scanning confocal microscopy (Leica TCS NT, Leica, Germany).

## 3. Results and discussion

### 3.1. Synthesis and characterization of the block copolymer

A molecular weight of the PIPAM-*b*-PBMA block copolymers were estimated from characterization of each polymer chain. Results are summarized in Table 1. For the P(IPAM–DMAM)-*b*-PLA block copolymers, molecular weights and polydispersities (PDI) were determined by GPC, and its molar ratios of IPAM, DMAM, and LA units were determined with a $^1H$ NMR spectrum using $CDCl_3$ as a solvent. Results are summarized in Table 2. Chemical structures of the block copolymers are shown in Fig. 1.

### 3.2. Characterization of polymeric micelles

Core-shell type micelle formation through self-association of the amphiphilic diblock copolymers and doxorubicin (DOX) loading were successfully achieved by dialysis of the polymer/drug mixtures in organic solvents against water at a temperature below the LCST of shell-forming polymer segments. For the PIPAM/PBMA micelles, a high DOX loading content (9.6 wt%) was obtained. The hydrodynamic diameters of the DOX-loaded PIPAM/PBMA micelles showed a relatively large distribution (338 nm, Fig. 2(a)). In general, particle size of mono-dispersed (not aggregated) polymeric micelle is known as 10–200 nm [5]. This larger particle size of the PIPAM/PBMA micelles was considered to be caused by the aggregation of individual polymeric micelles. On the other hand, a relatively low DOX incorporation (4.4 wt%) was obtained for the P(IPAM–DMAM)/PLA micelles. A possible explanation for a lower DOX content in the P(IPAM–DMAM)/PLA micelle is as the follows; (a) The PBMA inner cores possess higher hydrophobicity than the PLA cores due to hydrophobic butyl side chains, and (b) the crystalline structure of PLA inhibits the DOX entrapment in the inner cores. The averaged diameter of DOX-loaded P(IPAM–DMAM)/PLA micelles was 135 nm in a typical range of dispersed polymeric micelles (Fig. 2(b)). This result was probably due to that successful structural stabilization of thermoresponsive micelles was achieved by introduction of hydrophilic comonomer, DMAM into PIPAM main chains. For passive targeting using particles, their nano-ordered sizes (5–200 nm) are a very important factor for long circulation in the blood stream, avoiding from RES uptake [4], and allowing for selective tumor targeting due to the EPR effect of solid tumors. The prepared P(IPAM–DMAM)/PLA micelles have appropriate particle sizes with highly dispersed, non-aggregating properties, indicating their utility as targeted carrier systems.

The LCST of the DOX-loaded micelles were investigated by a turbidity method. In our previous works, it was clearly demonstrated that the hydrophilic or hydrophobic contribution to the LCST of PIPAM was particularly high when such groups were located at termini of the PIPAM chains [19,20]. The obtained hydroxyl-terminated PIPAM (PIPAM–OH) exhibited higher LCST of 34.5 °C in water than IPAM homopolymers prepared by conventional radical polymerization (32 °C). This

Table 1
Characterization of PIPAM-*b*-PBMA and the DOX-loaded micelles

| Mw (PIPAM–OH)[a] | Mn (PBMA–COOH)[b] | LCST (°C)[c] | DOX content (wt%) |
|---|---|---|---|
| 6100 | 8900 | 32.5 | 9.6 |

[a] Mw of PIPAM was determined by GPC in DMF with 10 mM LiCl.
[b] Mn of PBMA was estimated by end-group assay.
[c] Determined by transmittance changes in water.

result was considered that large hydrophilic contribution was enhanced by introduction of the terminal hydroxyl group in PIPAM due to stronger hydrogen bonding with water. However, the micelles comprising PIPAM-*b*-PBMA block copolymers showed the same LCST of unmodified IPAM homopolymers, irrespective of hydrophobic PBMA co-introduction. We have previously reported that thermoresponsive polymeric micelles comprising AB block copolymers of the PIPAM segment and a hydrophobic segment showed an LCST of 32.5 °C, identical to that of the IPAM homopolymer due to a clearly phase-separated micelle structure between the hydrophilic outer shells and the hydrophobic inner cores [19,21]. Furthermore, we have successfully adjusted the LCST of polymeric micelles comprising P(IPAM–DMAM)-*b*-PLA block copolymers to a temperature (39.5 °C) which is slightly higher than the body temperature by introduction of DMAM into the PIPAM main chain. This P(IPAM–DMAM)/PLA micelle system can be useful for multi-targeting methodology in conjunction with the localized hyperthermia at 42 °C, tumors are attacked by both selective cytotoxic activity of drugs (control of timing and duration) and selective hyperthermia [22].

### 3.3. Intracellular drug distribution

Subcellular distributions of DOX as free drug or loaded in the polymeric micelles inside of the cultured MCF-7 cells were observed by fluorescence microscopy detecting DOX fluorescence (red color). The nuclei of MCF-7 cells were selectively visualized (blue color) by Hoechst 33258 stain (Fig. 3(a and g)). Un-incorporated free DOX was almost exclusively found in nuclei (Fig. 3(b–f)) for incubation periods of 1 h to 24 h. The accumulation of free DOX progressed at a very high rate and saturated at 3 h incubation. For longer incubation periods, nuclei red color did not change. This behavior was identical to results reported in other papers [23]. Then, it was shown that subcellular distribution of DOX was not affected by temperature change from 37 °C (Fig. 4(a)) to 29 °C (Fig. 4(b)). On the other hand, DOX-loaded in the PIPAM/PBMA micelle system (LCST: 32.5 °C) was allowed to be clearly detected at 3 h and later. The intensity of the DOX color kept increasing by 24 h at a slower rate than free DOX (Fig. 3(h–l)). For the micelles, DOX images were shown to be uniformly distributed in whole inside of cells at 37 °C (above the micelle LCST) after thoroughly rinsing the cells to remove the micelles adhered to the cell surfaces below the LCST (25 °C). These results suggested that drug

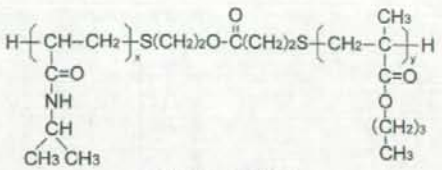


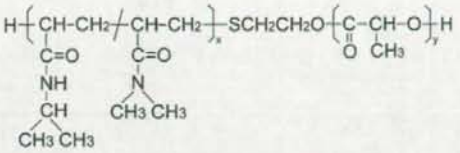


Fig. 1. Chemical structures of block copolymers.

Table 2
Characterization of P(IPAM–DMAM)-*b*-PLA and the DOX-loaded micelles

| P(IPAM–DMAM)-*b*-PLA (P(IPAM–DMAM)–OH)[a] | | Composition (molar ratio)[b] | | | LCST (°C)[c] | DOX content (wt%) |
|---|---|---|---|---|---|---|
| Mw[a] | PDI[a] | IPAM | DMAM | LA | | |
| 19600 (14800) | 1.42 (1.26) | 47 | 21 | 33 | 39.5 | 4.4 |

[a] Determined by GPC in DMF with 10 mM LiCl.
[b] Estimated by $^1$H NMR spectrum.
[c] Determined by transmittance changes in PBS.

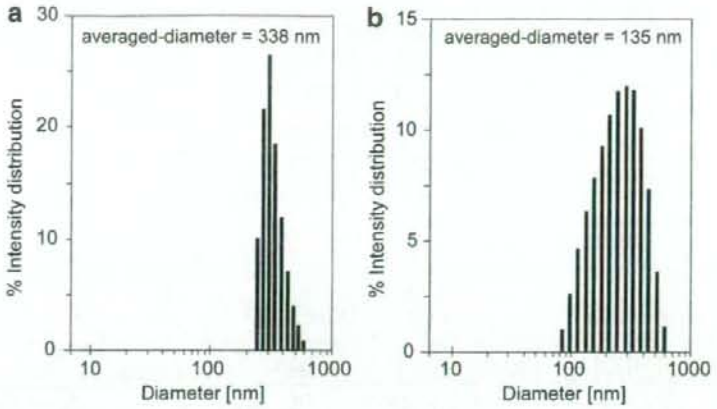


Fig. 2. Diameter distributions of (a) the DOX-loaded PIPAM/PBMA micelles and (b) the DOX-loaded P(IPAM–DMAM)/PLA micelles.

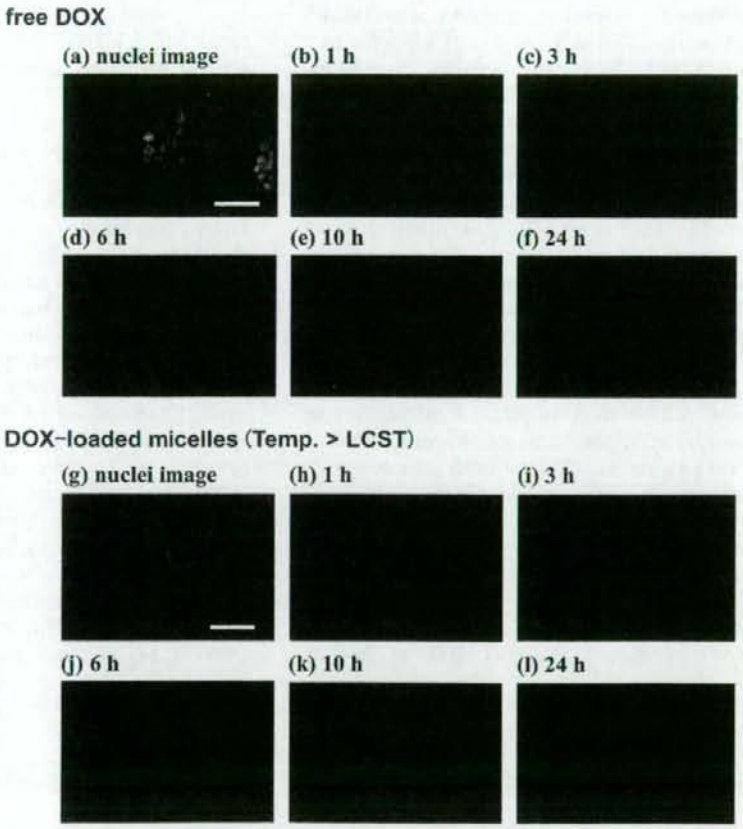


Fig. 3. Intracellular localization of free DOX and DOX-loaded in the PIPAM/PBMA micelles in MCF-7 cells. (a) nuclei stained with Hoechst 33258. Incubation for (b) 1 h, (c) 3 h, (d) 6 h, (e) 10 h and (f) 24 h with 30 μg/ml free DOX at 37 °C., (g) nuclei stained with Hoechst 33258. Incubation for (h) 1 h, (i) 3 h, (j) 6 h, (k) 10 h and (l) 24 h with 30 μg/ml DOX-loaded in the PIPAM/PBMA micelles at 37 °C. Bar represents 50 μm.

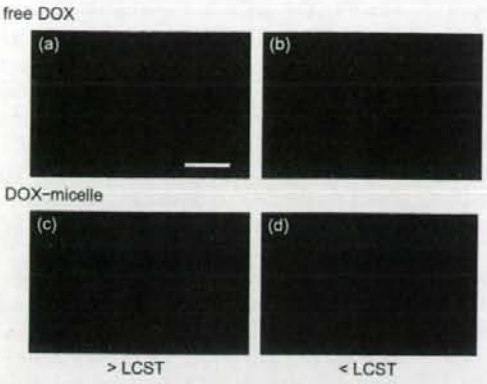


Fig. 4. Temperature effects on intracellular localization of DOX in MCF-7 cells.: Incubation for 6 h with 30 μg/ml free DOX at (a) 37 °C and (b) 29 °C. Incubation for 24 h with 30 μg/ml DOX loaded in the PIPAM/ PBMA micelles at (c) 37 °C and (d) 29 °C. Bar represents 50 μm.

delivery mechanism into the cells was different between free DOX and the DOX-loaded in the polymeric micelles. It is considered that DOX entered the cells in a micelle form, since its uniform distribution was totally different from free DOX distribution shown above. We have previously investigated temperature-modulated cellular uptake of fluorescein-labeled thermoresponsive micelles (averaged diameter: 30 nm) using cultured bovine endothelium cells by confocal laser scanning microscopy and flow cytometry [24]. Only above the micelle LCST, the micelles were significantly observed inside of the cells and localized around the nuclei. Furthermore, we have successfully achieved ON–OFF controlled intracellular uptake of the micelles via heating-cooling cycles across the micelle LCST. The drugs located at the nuclei using the micelles were probably due to accumulation of the released DOX from the micelles. In our previous report, the PIPAM/PBMA micelles exhibited approximately 90% DOX released against total loading content in PBS after 24 h above the LCST [15]. Of interest, as compared with images obtained above the LCST of the micelle (37 °C), the amount of DOX delivered to the cells drastically decreased below the LCST (29 °C) (Fig. 4(c and d)). This significant temperature effect indicated that hydrophilic PIPAM outer shells below its LCST lowered interactions with cell surfaces due to their highly hydrated shells. Upon the temperature raise above the micelle LCST, the outer shells switches their properties from hydrophilic to hydrophobic, and then the hydrophobic interactions between the micelles and the cell were consider to increase. Consequently, adhesion of the polymeric micelles was promoted, followed by significant enhancement of cellular uptake. Above the LCST, PIPAM-brush interfaces actively interact with biocomponents such as cells and proteins, whereas the surfaces changed into hydrated state with inhibiting these interactions below the LCST. Indeed, we have already demonstrated the PIPAM-grafted interfaces with a hydrophilic/hydrophobic switchable character for various applications including novel aqueous chromatography systems to separate bioactive compounds [25,26] and thermally regulated cell adhesion and detachment controlled solely by temperature changes [27,28].

We further investigated intracellular drug delivery *via* the thermoresponsive polymeric micelles using doxorubicin-resistant MCF-7 cell line (MCF-7/DOX). Free DOX was demonstrated much lower intracellular distribution in the resistant cells than its parent sensitive MCF-7 (Fig. 4(a) and Fig. 5(a)). This decrease is considered to result from efflux pump activity of the resistant cells. Interestingly, for the PIPAM/PBMA polymeric micelles above the micelle LCST, strong DOX fluorescence was observed in the DOX-resistant cells, irrespective of drug efflux activity. The extent of DOX intensity decreased only slightly compared with the DOX-

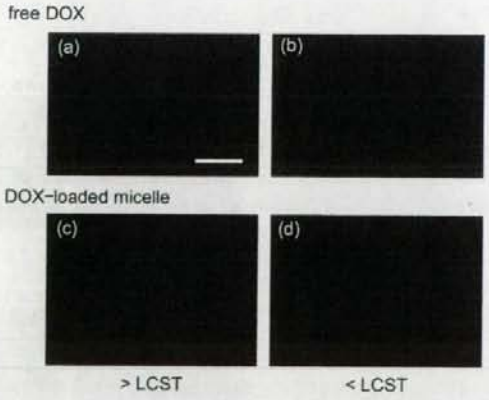


Fig. 5. Differences in intracellular localization between free DOX and DOX-loaded in the polymeric micelles in MCF-7 DOX resistant cells. Incubation for 6 h with 30 μg/ml free DOX at (a) 37 °C and (b) 29 °C. Incubation for 24 h with 30 μg/ml DOX-loaded in the PIPAM/PBMA micelles at (c) 37 °C and (d) 29 °C. Bar represents 50 μm.

sensitive cells (Fig. 4(c) and Fig. 5(c)). At the temperature below the LCST, the fluorescence intensity of DOX using the polymeric micelles was very small in this MCF-7/DOX. These results indicated that accumulation of free DOX was greatly inhibited in the resistant cell due to its resistant mechanism, and that a very large amount of drugs were delivered into the DOX-resistant cells utilizing thermal triggered micelle system. Consequently, we might accomplish to deliver anti-cancer drugs into MCF-7/DOX cells efficiently to overcome multi-drug resistant activity, and a novel strategy of cancer chemotherapy can be developed using the thermoresponsive micelle drug carrier system.

Biodegradable characters of the core-forming segments are preferable since the polymers obtained after the degradation (their molecular weights are below the critical value of ca. 40,000) can be rapidly excreted from the body through the renal excretion [29]. In addition, the thermoresponsive polymeric micelles with controlled higher LCST than human body temperature can be utilized for tumor hyperthermic treatment. Hyperthermia is known that exposure of high temperatures (around 42 °C) damages and kills cancer cells without biological damage to normal cells [22]. Therefore, we designed and prepared the P(IPAM–DMAM)/PLA micelles which possess both biodegradable properties of PLA inner cores and the controlled LCST value of 39.5 °C for the combination with the localized hyperthermic therapy. Intracellular distribution of free DOX at 37 °C and 42.5 °C was found to be effective the same as those in the experiment mentioned above (Fig. 3(b–f)). Free DOX was selectivity found in cell nuclei, and its red color was saturated at 6 h because no change was seen at 10 h and 24 h (data not shown). No temperature effect was observed between 37 °C and 42.5 °C. For the DOX-loaded in the P(IPAM–DMAM)/PLA micelles, the DOX accumulation in MCF-7 is much slower than free drug, it increased by 24 h incubation in a time-dependent manner (Fig. 6). In addition, the significant temperature effect of DOX accumulation across its LCST was clearly demonstrated using the thermoresponsive micelles. After 24 h incubation, a much larger amount of DOX in the cell above the LCST was detected than that below the LCST (Fig. 6(f and h)). In the P(IPAM–DMAM)/PLA micelle system, we also successfully controlled the critical temperature of intracellular drug delivery higher body temperature by LCST regulation of shell-forming polymer chains *via* hydrophilic DMAM introduction. Therefore, efficient tumor treatments can be obtained using thermoresponsive micelle drug carrier system in conjunction with local heating; tumor tissues are attacked by both selective cytotoxic activity of drugs and selective hyperthermia (42 °C). These phenomena of drug distribution using the thermoresponsive micelles were scarcely affected on differences in chemical components of block copolymers between two types of the micelles.

In order to confirm intracellular localization of free DOX and DOX loaded in the micelles, we

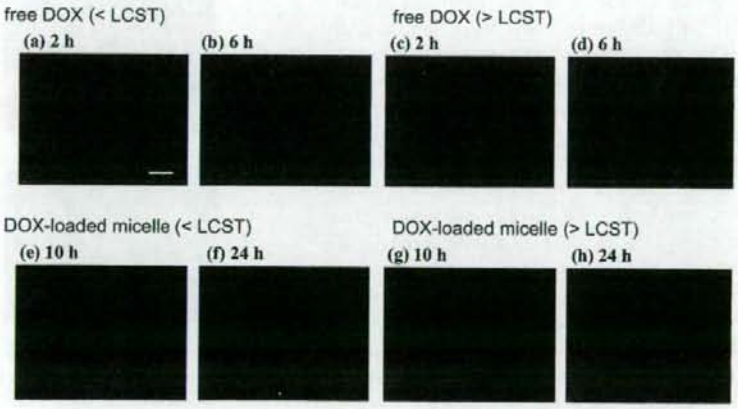


Fig. 6. Intracellular localization of free DOX and DOX-loaded in the P(IPAM–DMAM)/PLA micelles in MCF-7 cells. Incubation with 30 μg/ml free DOX for 6 h at (a) 37 °C and (b) 42.5 °C. Incubation with 30 μg/ml DOX-loaded in the P(IPAM–DMAM)/PLA micelles for 10 h at (c) 37 °C and (d) 42.5 °C, for 24 h at (e) 37 °C and (f) 42.5 °C. Bar represents 50 μm.

observed confocal images of MCF-7 cells exposed to each DOX. Free DOX was found to accumulate in only the cell nuclei (Fig. 7(a)). Kiyokami et al. previously reported the mechanism of selective DOX accumulation in the cell nuclei [30]; cytoplasmic DOX-binding proteasomes selectively transport DOX from the cytoplasm to the nucleus. By contrast, subcellular distribution of DOX using the micelles was observed in whole cells above its LCST as shown in Fig. 7(b). DOX accumulated in the cell nuclei using the thermoresponsive micelles probably due to accumulation of released DOX from the micelles. The P(IPAM–DMAM)/PLA micelles previously demonstrated 10% released against total loading DOX after 2 days in PBS above the LCST [17]. These suggested that DOX was mainly delivered into the cells in micelle form, and was enhanced intracellular release trough triggered phase transition of the micelle outer shells. Fig. 8 illustrates active drug targeting using the thermoresponsive polymeric micelles. We have previously demonstrated a thermal cytotoxic regulation using the DOX-loaded thermoresponsive micelles against cultured cell lines [15,17]. Expression of drug activity is initiated by external supply of heat. A delivery way of drug mediated by the temperature changes is considered the following two modes; (a) Drugs are extracellularly released from the polymeric micelles and diffuse into the cells, and (b) the polymeric micelles are taken up by the cells, and drugs are intracellularly released. It can be determined by a balance between the drug release rate and the frequency of cellular uptake which way plays a major role.

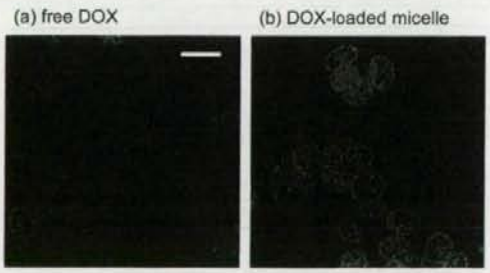


Fig. 7. Confocal images of free DOX and DOX-loaded in the P(IPAM–DMAM)/PLA micelles in MCF-7 cells. (a) Incubation with 30 μg/ml free DOX for 6 h at 42.5 °C, and (b) incubation with 30 μg/ml DOX-loaded in the P(IPAM–DMAM)/PLA micelles for 24 h at 42.5 °C. Bar represents 20 μm.

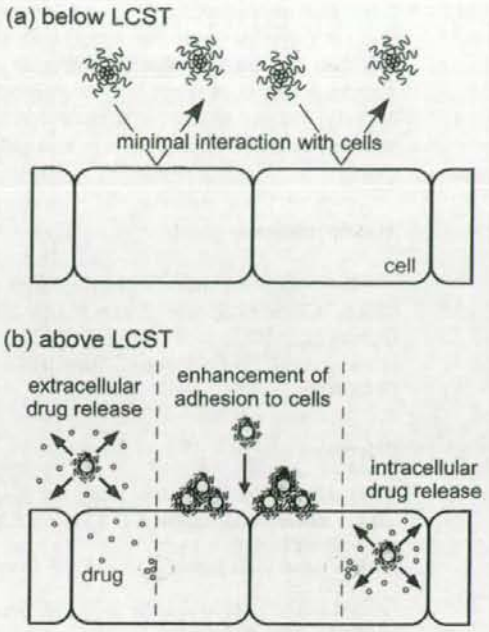


Fig. 8. Schematic mechanism of drug delivery to the target cells using the thermoresponsive polymeric micelles.

## 4. Conclusion

In this paper, we demonstrated the thermal modulation of intracellular drug distributions using the polymeric micelles with thermoresponsive outer shells comprising PIPAM or its copolymers. Unincorporated free DOX accumulated rapidly and selectively in cell nuclei without any temperature effects. By contrast, the distributions of DOX-loaded in the thermoresponsive micelles inside of the MCF-7 cells showed a significant temperature effect. DOX delivered by the micelles distributed uniformly in whole cells above the micelle LCST, while slight DOX accumulation was showed in the cell below the LCST. Interestingly, the DOX-loaded polymeric micelles exhibited a completely different behavior from free DOX in DOX-resistant MCF-7 cells. Although free DOX was detected slightly in the DOX resistant cells, the DOX-loaded in the micelles accumulated considerably above the LCST, irrespective of drug resistant activity. The thermal modulations of intracellular drug delivery using the thermoresponsive micelles also successfully achieved around human body temperature *via*

controlled micelle LCST (39.5 °C) for the combination with hyperthermic therapy. These results suggest that our thermoresponsive micelle system has a great potential in regulation of intracellular drug delivery against cancer cells including multi-drug resistant cells as well as for a multi-targeting cancer therapy.

## Acknowledgement

This work was supported by the Ministry of Education, Culture, Sports, Science and Technology, Japan (a Millennium Project No. 12415 and Grant-in-Aid for Young Scientists (B) No. 19700407).

## References

[1] D. Putnum, J. Kopecek, Adv. Polym. Sci. 122 (1995) 55.
[2] R. Duncan, S. Dimitrijevic, E.G. Evagoroa, S.T.P. Pharma. Sci. 6 (1996) 237.
[3] P.G. Tardi, N.L. Boman, P.R. Cullis, J. Drug Targeting 4 (1996) 129.
[4] O. Ishida, K. Maruyama, K. Sasaki, M. Iwatsuru, Int. J. Pharm. 190 (1999) 49.
[5] G.S. Kwon, K. Kataoka, Adv. Drug Deliv. Rev. 16 (1995) 295.
[6] Z. Tuzar, P. Kratochvil, Adv. Colloid Interf. Sci. 6 (1976) 201.
[7] M. Wilhelm, C. Zhao, Y. Wang, R. Xu, M.A. Winnik, J. Mura, G. Riess, M.D. Croucher, Macromolecules 24 (1991) 1033.
[8] Y. Matsumura, H. Maeda, Cancer Res. 46 (1986) 6387.
[9] H. Maeda, L.W. Seymour, Y. Miyamoto, Bioconjugate Chem. 3 (1992) 351.
[10] G.S. Kwon, S. Suwa, M. Yokoyama, T. Okano, Y. Sakurai, K. Kataoka, J. Control. Release 29 (1994) 17.
[11] M. Yokoyama, T. Okano, Y. Sakurai, S. Fukushima, K. Okamoto, K. Kataoka, J. Drug Targeting 7 (1999) 171.
[12] M. Nakayama, T. Okano, J. Drug Deliv. Sci. Tech. 16 (2006) 35.
[13] Z.-G. Gao, H.D. Fain, N. Rapoport, J. Control. Release 102 (2005) 203.
[14] K. Na, E.S. Lee, Y.H. Bae, J. Control. Release 87 (2003) 3.
[15] J.E. Chung, M. Yokoyama, M. Yamato, T. Aoyagi, Y. Sakurai, T. Okano, J. Control. Release 62 (1999) 115.
[16] F. Kohori, K. Sakai, T. Aoyagi, M. Yokoyama, Y. Sakurai, T. Okano, J. Control. Release 55 (1998) 87.
[17] F. Kohori, K. Sakai, T. Aoyagi, M. Yokoyama, M. Yamato, Y. Sakurai, T. Okano, Colloids Surf. B: Biointerf. 16 (1999) 195.
[18] M. Heskins, J.E. Guillet, J. Macromol. Sci. Chem. A2 (1968) 1441.
[19] J.E. Chung, M. Yokoyama, T. Aoyagi, Y. Sakurai, T. Okano, J. Control. Release 53 (1997) 119.
[20] J.E. Chung, M. Yokoyama, K. Suzuki, T. Aoyagi, Y. Sakurai, T. Okano, Colloids Surf. B: Biointerf. 9 (1997) 37.
[21] S. Cammas, K. Suzuki, Y. Sone, Y. Sakurai, K. Kataoka, T. Okano, J. Control. Release 48 (1997) 157.
[22] A.M. Ponce, Z. Vuujaskovic, F. Yuan, D. Needham, M.W. Dewhirst, Int. J. Hyperthermia 22 (2006) 205.
[23] O. Hovorka, M. St'astny, T. Etych, V. Subr, J. Strohalm, K. Ulbrich, B. Rihova, J. Control. Release 80 (2002) 101.
[24] J. Akimoto, M. Nakayama, K. Sakai, T. Okano, Submitted for publication.
[25] H. Kanazawa, T. Sunamoto, Y. Matsushima, A. Kikuchi, T. Okano, Anal. Chem. 72 (2000) 5961.
[26] J. Kobayashi, A. Kikuchi, K. Sakai, T. Okano, Anal. Chem. 73 (2001) 2027.
[27] T. Okano, N. Yamada, H. Sakai, Y. Sakurai, J. Biomed. Mater. Res. 27 (1993) 1243.
[28] T. Okano, N. Yamada, M. Okuhara, H. Sakai, Y. Sakurai, Biomaterials 16 (1995) 297.
[29] L.W. Seymour, R. Duncan, J. Strohalm, J. Kopecek, J. Biomed. Mater. Res. 21 (1987) 1341.
[30] K. Kiyokami, S. Matsuo, M. Kurebe, Cancer Res. 61 (2001) 2467.

# Synthesis and Characterization of a Temperature-responsive Amphiphilic Block Copolymer Containing a Liquid Crystalline Unit

Masamichi Nishihara,[1] Yoshihiko Murakami,[2] Takashi Shinoda,[3] Jun Yamamoto,[3] and Masayuki Yokoyama*[1]
[1]*Kanagawa Academy of Science and Technology (KAST), KSP East 404, 3-2-1 Sakado, Takatsu, Kawasaki 213-0012*
[2]*Department of Organic and Polymer Materials Chemistry, Tokyo University of Agriculture and Technology, 2-24-16 Nakacho, Koganei, Tokyo 184-8588*
[3]*Department of Physics, Graduate School of Science, Kyoto University, Kita-Shirakawa, Kyoto 606-8502*

(Received September 12, 2008; CL-080873; E-mail: yp-yokoyama2093ryo@newkast.or.jp)

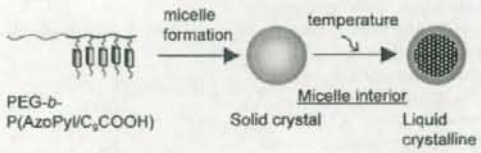


REPRINTED FROM

Chemistry Letters

Vol.37 No.12 2008 p.1214–1215
CMLTAG
December 5, 2008

The Chemical Society of Japan

Published on the web (Advance View) November 1, 2008; doi:10.1246/cl.2008.1214

# Synthesis and Characterization of a Temperature-responsive Amphiphilic Block Copolymer Containing a Liquid Crystalline Unit

Masamichi Nishihara,[1] Yoshihiko Murakami,[2] Takashi Shinoda,[3] Jun Yamamoto,[3] and Masayuki Yokoyama*[1]
[1]*Kanagawa Academy of Science and Technology (KAST), KSP East 404, 3-2-1 Sakado, Takatsu, Kawasaki 213-0012*
[2]*Department of Organic and Polymer Materials Chemistry, Tokyo University of Agriculture and Technology, 2-24-16 Nakacho, Koganei, Tokyo 184-8588*
[3]*Department of Physics, Graduate School of Science, Kyoto University, Kita-Shirakawa, Kyoto 606-8502*

(Received September 12, 2008; CL-080873; E-mail: yp-yokoyama2093ryo@newkast.or.jp)

To create a stimuli-responsive micelle, we synthesized a novel temperature-responsive amphiphilic block copolymer, poly(ethylene glycol)-*block*-poly{6-[4-(4-pyridylazo)phenoxy]-hexyl methacrylate} [PEG-*b*-P(AzoPyl)], by undertaking the RAFT polymerization of an AzoPyl monomer with a PEG macro-RAFT reagent. This block copolymer possesses a liquid crystalline unit derived from a hydrophobic AzoPyl/carboxylic acid complex. The PEG-*b*-P(AzoPyl/decanoic acid ($C_9COOH$)) complex formed a micelle structure (weight-average diameter = 68 nm). DSC results confirmed that the PEG-*b*-P(AzoPyl/$C_9COOH$) micellar solution exhibited thermodynamic phase-transition behavior.

Stimuli-responsive polymeric materials such as polymeric micelles[1] and liposomes[2] can serve as drug carriers for drug-delivery systems, which release loaded drugs by means of external stimuli. The drug release triggered by the external stimuli at tumor sites is a very important technology for targeted cancer chemotherapy, resulting in both a high local drug concentration at the tumor sites and a suppression of toxic side effects at the normal organs and tissues. In this study, we applied liquid crystalline polymers (LCPs)—functioning as a temperature-responsive moiety—to the interior of polymeric micelles. This study uses as its liquid crystalline (LC) moiety an azopyridyl group that exhibits the ability to control the LC phase-transition characteristics by means of a simple complexation of carboxylic acids without any synthetic modifications. Introduction of the LC unit to the interior of the polymeric micelle allows for the phase transition of the micelle inner core between the LC phase and the solid crystalline phase. Compared to the rigid solid state of the core, the highly fluid character of the LC phase may enhance incorporation of hydrophobic drugs into the core. Moreover, it is possible to stably retain the incorporated drugs by lowering the temperature below the phase-transition temperature, since the solid inner core is expected to inhibit the drug release from the inner core. Therefore, highly efficient and stable drug incorporation in polymeric micelles is feasible by the use of LCPs.

For this purpose, we synthesized poly(ethylene glycol)-*block*-poly{6-[4-(4-pyridylazo)phenoxy]hexyl methacrylate} (PEG-*b*-P(AzoPyl)) by undertaking the RAFT polymerization of 6-[4-(4-pyridylazo)phenoxy]hexyl methacrylate (AzoPyl) (Figure 1). AzoPyl served as a monomer with poly(ethylene glycol)-4-cyano-4-[(thiobenzoyl)sulfanyl]pentanoate (PEG dithiobenzoate) serving as a marco-RAFT reagent. AzoPyl[3] and PEG dithiobenzoate[4] were prepared according to a previously reported method. AzoPyl and PEG dithiobenzoate were dissolved in a mixture of anhydrous THF and DMSO, to which an AIBN

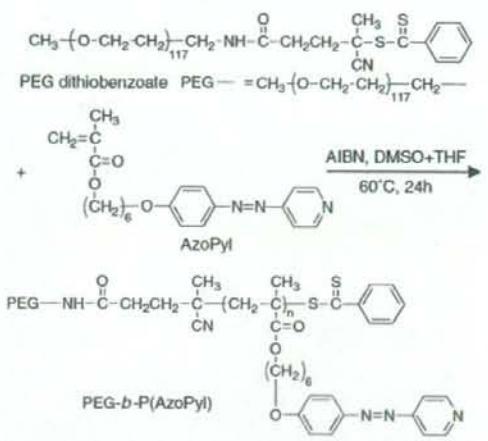


**Figure 1.** RAFT polymerization of AzoPyl with PEG dithiobenzoate.

DMSO solution was added. After five freeze–pump–thaw cycles, the solution was sealed in a vacuum, and the mixture was stirred at 60 °C for 24 h. The reaction mixture was poured into diethyl ether, and the precipitated polymer was dried in vacuo. Polymerization conditions are summarized in Table S1.[7]

RAFT polymerization was first tried in a dry DMSO solution.[5] However, the solubility of PEG dithiobenzoate in DMSO was low. To dissolve PEG dithiobenzoate well, we selected THF, which is a common solvent for a normal radical polymerization of AzoPyl homopolymers.[3] However, the monomer conversion in THF after 24 h was only 10% from $^1$H NMR. In order to solve this low-conversion problem and this solubility problem, we used a mixture of DMSO and THF. As expected, the monomer conversion of the polymerization in the DMSO/THF mixture increased up to 53%. The molecular weight (MW) of the obtained polymer 5-16 was 11300 (MW of PEG dithiobenzoate: 5500; degree of polymerization: 16). These findings indicate that the DMSO/THF mixture was a proper solvent system for the preparation of PEG-*b*-P(AzoPyl) by RAFT polymerization.

As shown in Figure S2[7] the GPC measurement of 5-16 shows that the peak not only completely shifted to an area of high molecular weight but also remained narrow (PDI = 1.09), indicating that this RAFT polymerization proceeded well.

We carried out an ATRP of the AzoPyl as well. Reaction conditions are described in the Supporting Information section.[7]

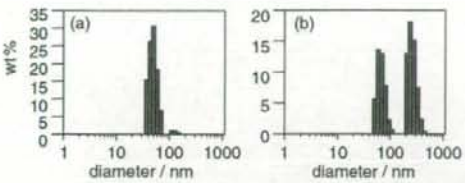


**Figure 2.** Size distributions of (a) the PEG-*b*-P(AzoPyl) (5-11) micelle and (b) the PEG-*b*-P(AzoPyl/$C_9$COOH) (5-11) micelle as determined by DLS.

However, no peak of the AzoPyl unit in the $^1$H NMR spectrum was observed, whereas peaks of the PEG initiator were found. A basic pyridyl group in the AzoPyl unit was expected to disturb the activity of the ATRP catalyst.

The capability of micelle formation is an important function for drug carriers. To confirm the existence of micelle formation, we used PEG-*b*-P(AzoPyl) (5-11, MW: 9400; degree of polymerization: 11), which had a composition similar to that of 5-16. Hydration of 5-11 was carried out by means of sonication.[6] To introduce the LC phase-transition function into the micellar core, PEG-*b*-P(AzoPyl) was complexed with decanoic acid ($C_9$COOH). DLS results of the PEG-*b*-P(AzoPyl) micellar solution indicate that two different-size types of particles, a 51 nm micelle and a 110 nm micelle, were distributed in the solution (Figure 2a). We considered that the smaller diameter was derived from a spherical micelle structure, and that the larger diameter was derived from a secondary associate of the spherical micelles. The PEG-*b*-P(AzoPyl/$C_9$COOH) micelle solution exhibited a similar distribution, 68 and 270 nm (Figure 2b). These results confirm that PEG-*b*-P(AzoPyl/$C_9$COOH) exhibited micelle-forming behavior similar to that of PEG-*b*-P(AzoPyl). Other DLS data are summarized in Table S2.[7]

Using DSC, we analyzed the thermal properties of PEG-*b*-P(AzoPyl/$C_9$COOH) (5-11) (Figures 3a and 3c). DSC curves of bulk PEG-*b*-P(AzoPyl) showed only endothermic and exothermic peaks associated with the melting and crystallization of the PEG unit, respectively (Figures 3b and 3d). In contrast, small exothermic peaks from 55 to 42 °C were observed in a cooling process that the PEG-*b*-P(AzoPyl/$C_9$COOH) complex underwent (Figure 3, inset). All DSC curves on the cooling process showed the same results in three-repeating measurements. It was reported that the AzoPyl homopolymer, complexed with $C_9$COOH, had its isotropic–smectic phase transition around 53 °C in cooling.[3] These results indicate that the AzoPyl/$C_9$COOH complex system exhibited the LC phase-transition behavior even in the PEG-*b*-P(AzoPyl) amphiphilic block copolymer. On the other hand, we observed no endothermic peak caused by the LC phase transition in heating. Probably, the endothermic peak of the LC phase transition overlapped the large peak of the PEG.

Observation of phase-transition behavior in a micellar interior is very attractive for stimuli-responsive polymeric micelles. Both the heating process and the cooling process of a PEG-*b*-P(AzoPyl/$C_9$COOH) micellar solution exhibited a small endothermic peak at 54 °C and a small exothermic peak at 43 °C (Figure S3[7]). In micellar solutions, the PEG chains are completely hydrated and unable to be crystallized; thus, the outer shell does not exhibit the phase transition. From these facts, we consider that the endothermic peak observed at 54 °C indicates phase transition in the micellar interior of PEG-*b*-P(AzoPyl/$C_9$COOH). On the other hand, the micelle's exothermic peak at 43 °C corresponded to the bulk sample's peaks ranging from 55 to 42 °C, indicating that the exothermic peak of the micelle might have derived from the LC phase transition of AzoPyl/$C_9$COOH. These DSC results of the micellar solution samples imply that the PEG-*b*-P(AzoPyl/$C_9$COOH) micelle solution exhibited the phase-transition behavior in the micellar inner cores.

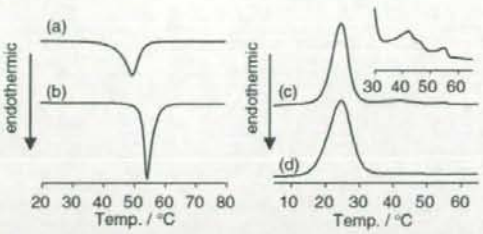


**Figure 3.** DSC curves (second scan) of bulk PEG-*b*-P(AzoPyl/$C_9$COOH) (5-11) ((a), (c)) and PEG-*b*-P(AzoPyl) (5-11) ((b), (d)). Here, (a) and (b) were in a heating process whereas (c) and (d) were in a cooling process. Inset shows exothermic peaks of PEG-*b*-P(AzoPyl/$C_9$COOH) from 30 to 65 °C in an expanded scale.

This polymeric micelle with the LC inner core may be very useful as a component of drug carriers. Furthermore, the nanosized LC inner core of the micelle is very interesting in regard to the physicochemical sciences. Regarding PEG-*b*-P(AzoPyl/carboxylic acid) complex micelles, future studies should investigate (1) control of drug incorporation, (2) drug release by temperature, and (3) possible evaluations of the LC phase transition in micellar inner cores.

This research was supported by the R&D project "Next-generation DDS Therapy Systems for Deep Therapy" undertaken by the New Energy and Industrial Technology Development Organization (NEDO).

**References and Notes**

1 a) M. Nakayama, T. Okano, T. Miyazaki, F. Kohori, K. Sakai, M. Yokoyama, *J. Controlled Release* **2006**, *115*, 46. b) E. S. Lee, K. Na, Y. H. Bae, *Nano Lett.* **2005**, *5*, 325. c) Y. Bae, N. Nishiyama, S. Fukushima, H. Koyama, Y. Matsumura, K. Kataoka, *Bioconjugate Chem.* **2005**, *16*, 122. d) M. Nakayama, T. Okano, *Macromolecules* **2008**, *41*, 504.
2 a) K. Kono, T. Murakami, T. Yoshida, Y. Haba, S. Kanaoka, T. Takagishi, S. Aoshima, *Bioconjugate Chem.* **2005**, *16*, 1367. b) L. Paasonen, B. Romberg, G. Storm, M. Yliperttula, A. Urtti, W. E. Hennink, *Bioconjugate Chem.* **2007**, *18*, 2131.
3 L. Cui, Y. Zhao, *Chem. Mater.* **2004**, *16*, 2076.
4 Y. Mitsukami, M. S. Donovan, A. B. Lowe, C. L. McCormick, *Macromolecules* **2001**, *34*, 2248.
5 L. Shi, T. M. Chapman, E. J. Beckman, *Macromolecules* **2003**, *36*, 2563.
6 M. Yokoyama, P. Opanasopit, T. Okano, K. Kawano, Y. Maitani, *J. Drug. Target.* **2004**, *12*, 373.
7 Supporting Information is also available electronically on the CSJ-Journal Web site, http://www.csj.jp/journals/chem-lett/index.html.

Published on the web (Advance View) November 1, 2008; doi:10.1246/cl.2008.1214

Journal of Controlled Release xxx (2009) xxx–xxx

Contents lists available at ScienceDirect

Journal of Controlled Release

journal homepage: www.elsevier.com/locate/jconrel

# Preparation and in vivo imaging of PEG-poly(L-lysine)-based polymeric micelle MRI contrast agents

Kouichi Shiraishi [a], Kumi Kawano [b], Takuya Minowa [b], Yoshie Maitani [b], Masayuki Yokoyama [a,*]

[a] Kanagawa Academy of Science and Technology, Yokoyama "Nano-medical Polymers" Project, KSP East 404, Sakado 3-2-1, Takatsu-ku, Kawasaki, Kanagawa 213-0012, Japan
[b] Institute of Medicinal Chemistry, Hoshi University, 2-4-41 Ebara, Shinagawa-ku, Tokyo 142-8501, Japan

ARTICLE INFO

*Article history:*
Received 24 October 2008
Accepted 17 January 2009
Available online xxxx

*Keywords:*
Polymeric micelle
MRI contrast agent
Long circulation
Tumor imaging
Poly(ethylene glycol)-b-poly(L-lysine)

ABSTRACT

A polymeric micelle drug carrier system was applied to the targeting of an MRI (magnetic resonance imaging) contrast agent. A block copolymer, PEG-*b*-poly(L-lysine), was used for conjugation of gadolinium ions through chelating moieties, DOTA. The DOTA moieties were successfully conjugated to all primary amine groups of the lysine residues. The obtained block copolymer, PEG-*b*-poly(L-lysine-DOTA), formed a polymeric micelle. The polymeric micelle structure was maintained even after partial gadolinium chelation (~40%) to the DOTA moieties. The prepared polymeric micelle MRI contrast agent was injected into a mouse tail vein at a dose of 0.05 mmol Gd/kg. The polymeric micelle-based MRI contrast agent exhibited stable blood circulation. A considerable amount (6.1±0.3% of ID/g of the polymeric micelle) was found to accumulate at solid tumors 24 h after intravenous injection by means of the EPR effect. An MRI analysis revealed that the signal intensity of the tumor was enhanced 2.0-fold by the use of this contrast agent.



## 1. Introduction

Various types of nano-sized drug carriers including linear synthetic polymers, dendrimers, proteins, liposomes, and polymeric micelles have been investigated for anti-cancer drug targeting to solid tumor sites for improvements in cancer chemotherapy [1,2]. Among these nano-sized carrier systems, polymeric micelles have been studied with a focus on encapsulation of hydrophobic drugs [3]. Most typically, polymeric micelles are constituted of block copolymers having a hydrophilic chain such as PEG and a hydrophobic chain. The hydrophobic chain can form a hydrophobic inner core that incorporates hydrophobic drugs. A strong advantage of the polymeric micelles is their high structural stability in the bloodstream and their very small size, being in a range of 10–100 nm. This size range is preferable for the passive targeting of solid tumors by means of the EPR (enhanced permeability and retention) effect [3]. Successful tumor-targeting-carrier systems include the adriamycin-incorporated polymeric micelle system [1], which involves a metal complex drug-incorporated (e.g., cisplatin-incorporated) polymeric system [4–6].

The recent study reported that several nano-sized-carrier system and, in particular, diagnostic imaging agents rest on drug-targeting methodology. Magnetic resonance imaging (MRI) is a non-invasive imaging modality for diagnosis. Owing to rapid developments in temporal and spatial resolution, the value of MRI has grown greater in recent decades. Nowadays, much attention is given to MRI contrast agents both of low molecular weight and of macromolecule status for their ability to improve MRI signals.

Paramagnetic metal complexes, such as the gadolinium (III) ion-DTPA complex, are widely used in clinical diagnosis. Such gadolinium complexes enhance $T_1$-weighted images by shortening the $T_1$-relaxation time of the water protons. Linear polymers such as dextran [7,8], poly(L-lysine) [9,10], poly(glutamic acid) [11–13], and poly[N-(2-hydroxypropyl)methacrylamide] [14] have been investigated as possible for carriers of the gadolinium complexes. Dendrimers, which possess well-defined structures and accurate molecular weights, have also attracted much attention as carriers of MRI contrast agents because dendrimers' biodistribution were depend on the generations [15–17].

Polymeric micelle-based MRI contrast agents also have a potential as MRI contrast agents. Because the polymeric micelle is an associate of many block copolymer chains, block copolymers with well-controlled molecular weight can be excreted through kidney filtration after dissociation of the polymeric micelles into block copolymer chains. Therefore, a low risk of chronic toxicity is expected to present itself and is expected to stem from polymeric micelles' complete excretion over a long time period. On the other hand, polymeric micelles can exhibit a preferential pharmacokinetic profile in a defined time period required for the targeting of tumors. In a previous report, we prepared a polyion complex micelle from charged block copolymers and counter ionic polymers [18]. This polymeric micelle MRI contrast agent possessed the characteristic of changeable $T_1$-relaxivity: The polymeric micelle exhibited a lower $T_1$-relaxivity than did block copolymer chains having dissociated from the micelle. This changeable character can be utilized as a tumor-specific MRI contrast

* Corresponding author. Tel.: +81 44 819 2093; fax: +81 44 819 2095.
*E-mail address:* yp-yokoyama2093ryo@newkast.or.jp (M. Yokoyama).

0168-3659/$ – see front matter © 2009 Elsevier B.V. All rights reserved.
doi:10.1016/j.jconrel.2009.01.010

with a high MRI contrast (in dissociate form) at tumor tissues and a low MRI contrast (in micelle form) in the bloodstream. In the previous report, we proved this changeable character in vitro, but did not examine in vivo tumor targeting.

Several works on polymeric micelles as MRI contrast agents were reported recently [19–22]. The combination of drug targeting and imaging probes, such as MRI contrast agents, relative to polymer micelles systems has strengthened the effectiveness of chemotherapy [23]. Poly(L-glutamic acid)-*b*-polylactide and polysuccinimidce derivatives were synthesized as a polymeric micelle-based MRI contrast agent [20,21]. Several studies have examined polymeric micelle-based MRI contrast agents, but so far, significant enhancements of MR images at solid tumors through accumulation of the polymeric micelles have not been obtained. One of the challenges that confront the use of MRI contrast agents to detect solid tumors is the selective delivery of the contrast agents to solid tumors by means of the EPR effect. From our experience of anti-cancer drug targeting with polymeric micelle carriers, we assume that an important key for successful tumor targeting is suppression of the incorporated drug's interactions with cells and proteins, in particular, hydrophobic interactions. In our previous report, we showed that polymeric micelles exhibiting lower levels of hydrophobic interactions provided higher levels of antitumor activities, possibly through more efficient passive targeting [24]. If this assumption is applied to MRI contrast agents, the micelle outer shell with a biologically inert character is preferable. Therefore, we have chosen a micelle design with the inert poly(ethylene glycol) outer shell and the contrast species (Gd ion)-containing inner core. Furthermore, we have chosen a negatively charged inner core, not a positively charged one, since positive charges are known to induce strong interactions with the reticuloendothelial system (RES) [25]. Consequently, strong interactions with the RES drastically lower the targeting efficiency relative to solid tumors.

In this report, we synthesized negatively charged block copolymers based on a poly(ethylene glycol)-*b*-poly(L-lysine) system to obtain a long-circulating polymeric micelle MRI contrast agent. This negatively charged block copolymer was found to form a polymeric micelle structure without an addition of positively charged macromolecules. Blood circulation, biodistribution, and excretion of the contrast agents were evaluated. MR images of mice were taken after an injection of the contrast agent, and these images were compared before the injection. According to the findings, polymeric-micelle MRI contrast agent appears to be a strong tool for polymeric-micelle-based drug targeting and for visualizing the location of the carriers at the solid tumor tissues.

## 2. Materials and methods

### 2.1. Materials

For the current study, α-methoxy-ω-aminopropyl-poly(ethylene glycol) (PEG-$NH_2$, $M_w$ = 5200) was purchased from NOF Corporation, Tokyo, Japan, and benzene-based lyophilization was carried out before use. A chelating agent active ester, 1,4,7,10-tetraazacyclododecane-1,4,7,10-tetraacetic acid mono (*N*-hydroxysuccinimide ester) (DOTA-OSu), was purchased from Macrocyclics, Texas, USA. Deuterium solvents were purchased from Sigma-Aldrich, Tokyo, Japan. Dehydrated DMF and gadolinium chloride hexahydrate ($GdCl_3$·$6H_2O$) were purchased from Wako Pure Chemicals Industries, Ltd., Tokyo, Japan. We used all these commercial reagents as purchased. The dialysis membrane Spectrapor 6 (molecular weight cut off (MWCO) = 1000) was purchased from Spectrum Laboratories Inc., Tokyo, Japan. $^1$H NMR spectra were recorded on a Varian UNITY INOVA 400 MHz NMR spectrometer. To measure gadolinium ion contents in the block copolymer, we used inductively coupled plasma (ICP) with an SPS7800 apparatus (SII NanoTechnology Inc., Tokyo, Japan). Dynamic

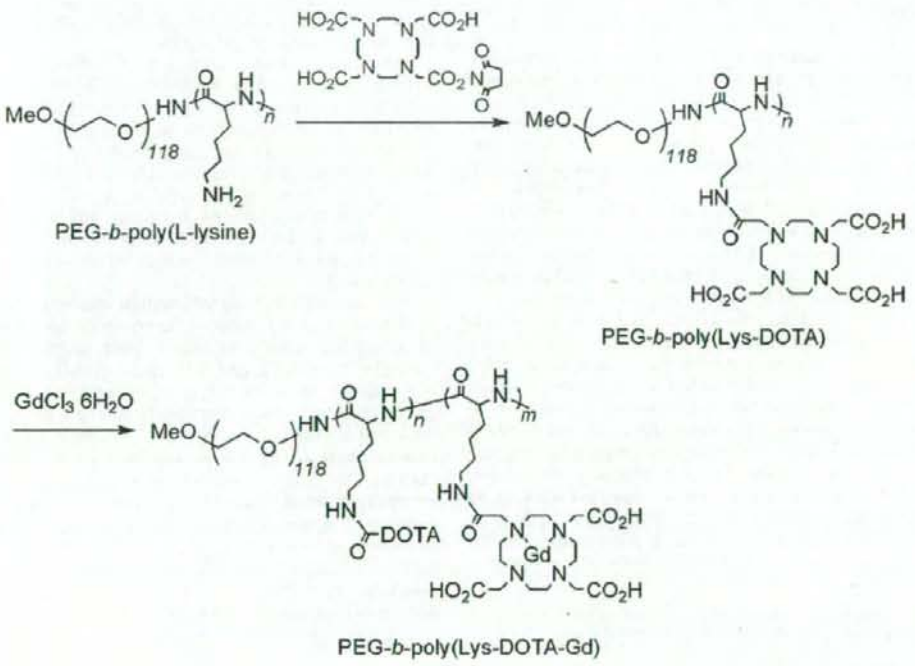


Fig. 1. Synthesis of PEG-P(Lys-DOTA-Gd).

Please cite this article as: K. Shiraishi, et al., Preparation and in vivo imaging of PEG-poly(L-lysine)-based polymeric micelle MRI contrast agents, J. Control. Release (2009), doi:10.1016/j.jconrel.2009.01.010

light scattering (DLS) measurements were carried out at 24.5 °C with a DLS-700 instrument (Otsuka Electronics Co., Ltd., Tokyo Japan). Measurement of zeta-potential was performed with an ELSZ-2 instrument (Otsuka Electronics Co., Ltd., Tokyo Japan).

### 2.2. Animals

Five-week-old ddY female mice and $CDF_1$ female mice were purchased from the Sankyo Labo Service Corporation, Tokyo, Japan. All animal experiments were carried out in accordance with the guidelines of the Guiding Principles for the Care and Use of laboratory Animals of Hoshi University.

### 2.3. Synthesis of PEG-P(Lys-DOTA)

A synthesis of a chelate moiety-binding block copolymer is shown in Fig. 1. A poly(ethylene glycol)-*b*-poly(L-lysine) block copolymer (PEG-P(Lys)) was prepared through acid hydrolysis of a poly(ethylene glycol)-*b*-poly[ε-(benzyloxycarbonyl)-L-lysine] (PEG-P(Lys(Z)) block copolymer [26]. We synthesized PEG-P(Lys)s from PEG-$NH_2$ (molecular weight of PEG-$NH_2$ = 5200). The compositions of PEG-P(Lys)s were determined by means of $^1H$ NMR in $D_2O$ under an acidic condition. A mixture of PEG-P(Lys) (86.0 mg), and 1,4,7,10-tetraazacyclododecane-1,4,7,10-tetraacetic acid mono (*N*-hydroxysuccinimide ester) (DOTA-OSu, 308.0 mg) in 8.6 mL of dry DMF was stirred, and then, dry triethylamine (0.5 mL) was added to this reaction mixture. The reaction mixture was stirred overnight at 50 °C. The resulting mixture was dialyzed, at first, against 0.02 N HCl and, then, against distilled $H_2O$ 5 times. The obtained polymer was dissolved in $H_2O$ (at a polymer concentration higher than 15 mg/mL) again, and dialyzed against $H_2O$ 3 times, and we obtained poly(ethylene glycol)-*b*-poly(L-lysine-DOTA) (PEG-P(Lys-DOTA)) by means of lyophilization (162.8 mg). The composition of PEG-P(Lys-DOTA) was determined by means of $^1H$ NMR in $D_2O$ under an alkali condition (pH > 10). The number of bound DOTA units per polymer chain was calculated from the peak area ratio among $CH_2$ protons of PEG at 3.73 ppm, 24H protons of DOTA, and 2H protons of lysine in the range of 3.36–2.18 ppm. $^1H$ NMR (ppm, $D_2O$ + NaOD): 4.08 (s, CH of lysine units), 3.73 (s, $CH_2$ of PEG), 3.39 (s, $OCH_3$ of terminal PEG), 3.36–2.18 (m, 24H of DOTA and $CH_2$ of lysine), and 2.18–1.10 (m, 6H of lysine).

### 2.4. Gadolinium (III) chelation to PEG-P(Lys-DOTA)

$GdCl_3$-$6H_2O$ (35.0 mg, 0.094 mmol) was added to PEG-P(Lys-DOTA) (153.3 mg) in $H_2O$ (15.0 mL), and the pH of the solution was maintained between 6.0–6.5. The reaction mixture was stirred for 3 h at 50 °C, followed by dialysis against distilled $H_2O$ 5 times. PEG-P(Lys-DOTA-Gd) was obtained as a white solid after lyophilization (160.8 mg). The determination of gadolinium ions in the block copolymer was carried out by means of ICP measurements (7.0 wt.%, the number of gadolinium ions per polymer chain was 6.7). The obtained PEG-P(Lys-DOTA-Gd) is indicated as 118-17-17-7 (PEG unit = 118, lysine units = 17, DOTA moieties = 17, number of gadolinium ion = 7).

### 2.5. Blood concentration of PEG-P(Lys-DOTA-Gd) micelles in mice

Blood samples (10–75 μL) from the tail vein ($n$ = 3) of mice (ddY) (30–33 g) were collected in heparinized capillary glass. Saline (1.5 mL) was added to the blood samples, and the mixture was centrifuged at 4 °C for 4 min at 13,000 rpm. The supernatant of the plasma solution was collected, and the gadolinium ion contents of the block copolymer were measured by means of ICP. The plasma and blood volume were calculated as 0.0488 mL/g body weight for plasma and 0.0778 mL/g body weight for blood, respectively.

### 2.6. Biodistribution of the contrast agents

Biodistribution of the contrast agents was evaluated in $CDF_1$ female mice (5 weeks old) (20–22 g) bearing a colon 26 tumor. Colon 26 cells ($1.0 \times 10^4$ cells/0.1 mL) were transplanted into $CDF_1$ female mice subcutaneously. Injection of the contrast agents was started 9–10 days after the transplantation. Tumor volumes were approximately 50–100 $mm^3$. The tumor volumes were calculated as follows: volume = $1/2LW^2$; $L$ is the long diameter and $W$ is the short diameter of a tumor.

Twenty-four hours after the injection, the blood was collected with a heparinized syringe and centrifuged at 4 °C for 4 min at 13,000 rpm. The plasma was obtained, and its gadolinium content was measured by means of ICP. The major tissues including tumor tissues were excised and weighted. For the determination of gadolinium ion content in the tissue, saline was added to the tissues, followed by an addition of nitric acid (conc. 70%) and sulfuric acid (conc. 98%). Then, the mixture was heated. A saturated aqueous oxoammonium solution was added to the yellow mixture and heated again. The resulting pale-yellow mixture was diluted with saline. The supernatant was collected, and its gadolinium content was measured by means of ICP. The urine ($n$ = 3) was collected 24 h and 48 h after injection, and its gadolinium content was measured by means of ICP.

### 2.7. MR imaging of mice tumor model

MR imaging was performed with female mice ($CDF_1$) bearing a colon 26 tumor. The tumor transplantation was carried out as described in 2.6. The contrast agents were injected at a dose of 0.05 mmol of Gd/kg into a mice-tail vein. MR images were taken with a Varian NMR system at 9.4 T. $T_2$-weighted fast spin echo (TR = 2500 ms, ETL = 8, ESP = 4, effective TE = 48) was performed for all experiments before following the $T_1$-weighted gradient echo protocol. $T_1$-weighted gradient echo protocol was followed before the injection, immediately after the injection, and then 4 h and 24 h after the injection. Imaging parameters of the $T_1$-weighted images were TR/TE = 8.0/4.2, flip angle = 30°, field of view of 50 × 30 mm, a matrix size of 192 × 192, and 2 mm of coronal slice thickness, and were TR/TE = 8.0/4.5, flip angle = 30°, field of view of 45 × 45 mm, a matrix size of 192 × 192, and 2 mm of axial slice thickness. For normalized signal intensity relative to the $T_1$-weighted images, the tumor area was selected as a region of interest (ROI). The signal intensity of the ROI was compared with the intensity of a stock solution of 0.1 mM gadolinium ion in agarose gel.

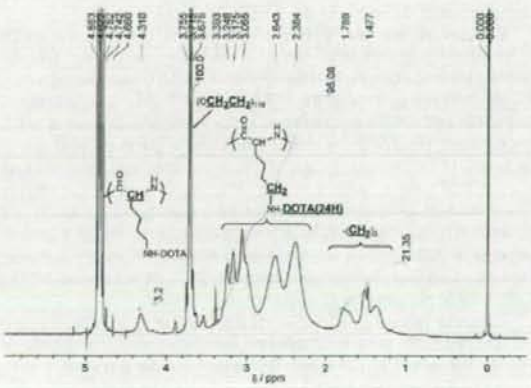


**Fig. 2.** $^1H$ NMR spectrum of PEG-P(Lys-DOTA) (118-17-17) in $D_2O$ + NaOD.

Please cite this article as: K. Shiraishi, et al., Preparation and in vivo imaging of PEG-poly(L-lysine)-based polymeric micelle MRI contrast agents, J. Control. Release (2009), doi:10.1016/j.jconrel.2009.01.010

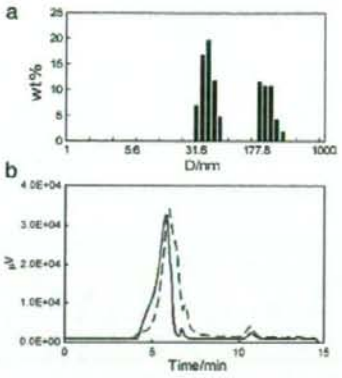


**Fig. 3.** (a) Weight–weight average size distribution of PEG-P(Lys-DOTA-Gd) micelle (118-17-17-7) in 150 mM NaCl measured by DLS, and (b) gel-permeation chromatogram of PEG-P(Lys-DOTA-Gd) micelle in $H_2O$ (1.2 mg/mL) of concentrated preparation of 118-17-17-7(solid line) and diluted preparation of 118-17-17-6 (dashed line).

The relative signal intensity of the ROI 24 h after the injection was compared with the signal intensity before the injection.

## 3. Results and discussion

### 3.1. Block copolymer synthesis and characterization of polymeric micelle

A block copolymer binding DOTA groups was synthesized from poly(ethylene glycol)-*b*-poly(L-lysine). The binding of a DOTA at the lysine residues was carried out with a coupling reaction between a primary amine and an NHS ester of a DOTA reagent, as shown in Fig. 1. Poly(ethylene glycol)-*b*-poly(L-lysine-DOTA) block copolymers possessing 5200 of molecular weights, and 17–21 units of the DOTA-bound lysine moiety were obtained. Quantitative substitution of lysine residues for DOTA was confirmed in $^1$H NMR spectra as shown in Fig. 2.

A fully DOTA-substituted block copolymer formed polymeric micelles after the dialysis in dist. $H_2O$ at a polymer concentration of 15 mg/mL. The quantitative DOTA conjugation was essential for the polymeric micelle formation. Insufficient DOTA conjugation, such as 118-22-19 wherein the number of DOTA residues was 19 out of 22 lysine residues, did not form a polymeric micelle. This result shows that the micelle structures were not formed in the presence of a small amount of unmodified lysine residue (3 out of 22 residues); the result also underscores the importance of strong interactions among the conjugation DOTA units for the micelle formation.

Gadolinium ion was partially chelated to DOTA in the block copolymer, poly(ethylene glycol)-*b*-poly(L-lysine-DOTA). Gadolinium-chelated poly(ethylene glycol)-*b*-poly(L-lysine-DOTA-Gd) maintained the polymeric micelle formation. Dynamic light scattering (DLS) and GPC measurements of the gadolinium chelated block copolymers, 118-17-17-7 which is 118 ethylene glycol units, 17 lysine residues, 17 DOTA conjugation to lysine residues, and 7 gadolinium ions at DOTA were performed. Fig. 3(a) shows a DLS chart of this block copolymer micelle with a weight average of 42.9±7.6 nm (mean±SD), accompanied by a secondary aggregation of a weight average of 225.5±53.0 nm (mean±SD). Similar secondary aggregation was also found in the precursor of PEG-*b*-poly(L-lysine-DOTA-Gd) (data in supplemental section).

The zeta-potential of the obtained polymeric micelle showed −9.55 mV in 150 mM NaCl solution, indicating that the polymeric micelle was negatively charged. This negative value was given from a vacant DOTA moiety having 3 carboxylic acids and 4 tertiary amines. The tertiary amines of DOTA could work as only two cationic species in the physiological condition owing to their excessively close proximity to each other, whereas three carboxylic acids in the DOTA moiety could work as 3 anions owing to their long distances from one other. As a result, the total charge of the polymeric micelles exhibited negatively charged particles. In general, cationic species are more quickly scavenged by the reticloendothelial system than anionic species [25]. This scavenging is a big obstacle for the passive tumor targeting through the EPR effect. For the design of a tumor-targeting system, a slightly negative-charged particle is preferable as an inert carrier.

GPC measurements of the polymeric micelle (1.2 mg/mL in $H_2O$) were performed by the use of an HPLC system (LC 2000 series, Jasco, Tokyo, Japan) equipped with a TSK-gel G4000-$PW_{XL}$ column (eluent=$H_2O$, flow rate=1.0 mg/mL, detector=RI) at 40 °C. Even in such a diluted aqueous solution of the block copolymer, both DLS and GPC measurements clearly exhibit the formation of the polymeric micelle as shown in Fig. 3(b) (solid line). This finding indicated that once the polymeric micelle was formed by interactions among vacant DOTAs, the polymeric micelle was not dissociated in a time scale of a DLS and GPC measurement under dilution. When we injected a similar sample 118-17-17-6 prepared from a dilute condition (3 mg/mL), the peak of the polymeric micelle was shifted to a longer elution time as shown in Fig. 3(b) (dashed line). This result indicates a considerable polymer concentration effect on the formation of the polymeric micelle; namely, strong interactions among vacant DOTA moieties at a high concentration.

Formation of the polymeric micelle with or without a gadolinium ion appears to depend on interactions among vacant DOTAs as described above. To prove this interaction, we added an excess of $GdCl_3$ (2.0 mol equivalent vs DOTA) into 118-20-20 to prepare complete chelation of the DOTA units with gadolinium ions. However, we found that the composition of the block copolymer was 118-20-20-16. Even when we added the excess amount of gadolinium ions to the block copolymer, we obtained 20% of vacant DOTA in the block copolymer. This result implies that DOTA–DOTA interactions prevent gadolinium ion from freely chelating into a DOTA moiety. When we injected this block copolymer into the GPC column, we observed that the peak of around 5–6 min. corresponded to the polymeric micelle disappeared. This disappearance indicates that chelation of a high level of gadolinium ion in a block copolymer resulted in so unstable micelle formation on the GPC column. We concluded that the polymeric micelle was formed through the interactions among vacant DOTAs, and that these interactions depend on the block copolymer concentrations and on the numbers of the chelated gadolinium ions.

### 3.2. Blood circulation of the polymeric micelle MRI contrast agent

The polymeric micelle, 118-17-17-7, was injected at a dose of 0.05 mmol Gd/kg, into a mouse-tail vein for pharmacokinetic

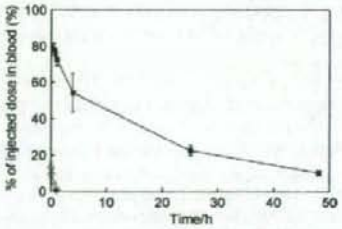


**Fig. 4.** Blood-concentration time course of PEG-P(Lys-DOTA-Gd) micelle (118-17-17-7) in ddY female mice at a dose of 0.05 mmol Gd/kg (■), and Gd–DTPA at a dose of 0.10 mmol Gd/kg (○). After defined time periods (0.5 h, 1 h, 2 h, 4 h, 24 h, and 48 h), the blood samples were collected into capillary glass tubes via mice's tail veins.

Please cite this article as: K. Shiraishi, et al., Preparation and in vivo imaging of PEG-poly(L-lysine)-based polymeric micelle MRI contrast agents, J. Control. Release (2009), doi:10.1016/j.jconrel.2009.01.010

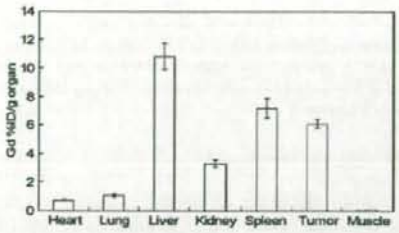


**Fig. 5.** Biodistribution of PEG-P(Lys-DOTA-Gd) micelle 24 h after injection at a dose of 0.05 mmol Gd/kg.

observations. The blood concentrations of the polymeric micelles were measured by means of ICP. Fig. 4 shows the blood concentration-time course of the polymeric micelles until 48 h after the injection. A low-molecular-weight gadolinium ion complex, such as Gd–DTPA, was immediately excreted 1 h after injection (only 1.4±0.8% was found in blood). On the other hand, the polymeric micelle remained 22.5±2.9% and 10.2±1.4% (mean±SD) in blood at 24 h and 48 h after the injection, respectively. These high blood concentrations exhibit significantly stable circulation of the polymeric micelle in blood. This polymeric micelle underwent an approximately 10-fold dilution relative to the injection in blood: however, stable formation of the polymeric micelle at such diluted conditions was confirmed in this in vivo experiment. This stable blood-circulation time-course was similar to the system of anti-cancer drug-incorporating polymeric micelle, a doxorubicin-incorporating poly(ethylene glycol)-*b*-poly (aspartic acid) system [1]. According to reports, the doxorubicin-incorporating polymeric micelle system provides a drug concentration of 24.6% of the injected dose (ID) after 24 h in the blood. Such a long circulating property of the doxorubicin-incorporating polymeric micelle successfully led to highly selective tumor accumulation. Owing to this similar pharmacokinetic behavior, this MRI contrast agent can be a strong tool for estimation of the pharmacokinetic behavior of "anti-cancer drug"-incorporating polymeric micelles.

### *3.3. Biodistribution and excretion of the polymeric micelle MRI contrast agent*

Selective and high accumulation of drug carriers at solid tumors is essential for an improvement of anticancer drug efficacy. As well as the drug-targeting systems, selective and high accumulation is desired for diagnostic agents.

In recent decades, polymeric micelles have constituted one of the best drug-carriers to have achieved selective accumulation of an anti-cancer drug, through the EPR effect, at solid tumor tissues [1]. Biodistribution of the polymeric micelle contrast agents was evaluated in $CDF_1$ female mice bearing the colon 26 tumor. Fig. 5 shows the percentage of the injected dose of the polymeric micelle 24 h after the injection in the normal organs as well as in tumor tissues. The study showed that the accumulation of the polymeric micelle contrast agent in tumor tissues reached 6.1±0.3% ID (injected dose)/g of tumor. This accumulation amount was considerably high. Furthermore, highly selective delivery was present with low accumulation amounts in heart, kidney, and muscle tissue. For the mononuclear phagocyte system (MPS), this contrast agent was found to be accumulated in 10.8±0.9 and 7.2±0.7% ID/g of liver and spleen, respectively. These accumulation ratios were similar to those in case of doxorubicin-incorporated polymeric micelle, but better tumor/muscle ratios were obtained in this MRI contrast agent [1]. This difference may rest on a difference in micelle size as well as in detection species: there is a physically entrapped drug for the drug-carrying micelles and there are chelated gadolinium ions for the MRI contrast agent. The gadolinium-binding macromolecular carrier may

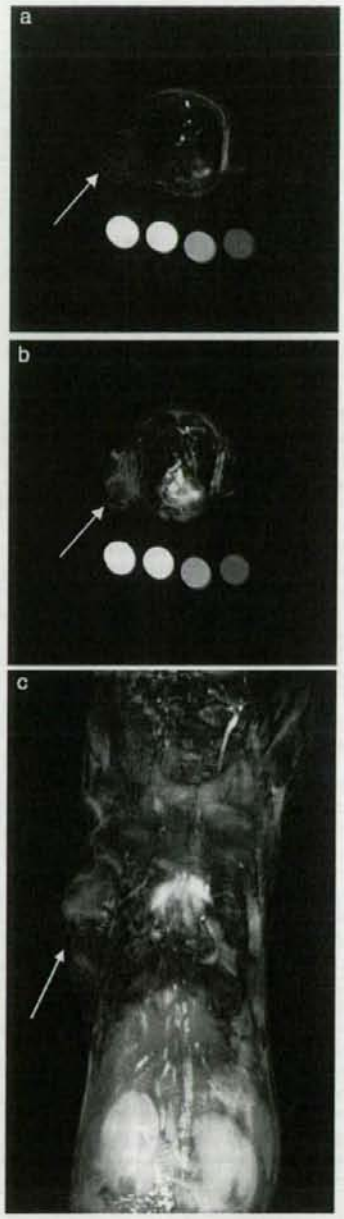


**Fig. 6.** Axial slices of MR images (a) before and (b) 24 h after the injection at a dose of 0.05 mmol Gd/kg. Tumor areas are on the left side in the axial slices. The circles indicate the stock solutions of (left to right) 1.0 mM, 0.5 mM, 0.1 mM gadolinium ion in agarose gel and blank in agarose gel. $T_1$-weighted gradient echo protocol was used. Parameters of the $T_1$-weighted images were TR/TE=8.0/4.5, flip angle=30°, field of view of 45×45 mm, a matrix size of 192×192, and 2 mm of axial slice thickness. Arrows indicate tumor tissue. (c) MIP images of coronal slices 24 h after injection. Arrow indicates tumor. Parameters of the $T_1$-weighted images were TR/TE=8.0/4.2, flip angle=30°, field of view of 50×30 mm, a matrix size of 192×192. MIP images were obtained by 2 mm thickness=4 slices.

Please cite this article as: K. Shiraishi, et al., Preparation and in vivo imaging of PEG-poly(L-lysine)-based polymeric micelle MRI contrast agents, J. Control. Release (2009), doi:10.1016/j.jconrel.2009.01.010

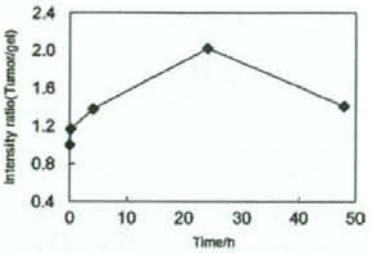


**Fig. 7.** Relative signal intensities of tumor area at defined time (0 h, 4 h, 24 h, 48 h) after the injection of the polymeric micelle MRI contrast agent.

not penetrate into muscle as do low-"molecular weight" drugs that are released from the carrier.

Wang Y et al. reported that poly[N-(2-hydroxypropyl)methacrylamide] (PHPMA) [14] gadolinium-conjugates exhibited size-dependent tumor accumulation. They stated that a large molecular weight of PHPMA (121 kDa) gadolinium conjugate exhibited the best tumor accumulation at 7 days after injection. Although, Bogdanov A et al. reported another example of successful passive targeting to solid tumors with a graft copolymer of poly(ethylene glycol) featuring poly(L-lysine) [9]. This contrast agent exhibited tumor targeting with a long blood-circulation time ($t_{1/2}$=36 h): however, this long-circulation property in blood indicates that the contrast agent cannot excrete smoothly from the body owing to the polymer's very large molecular weight (690 kDa). The researchers synthesized different molecular weights of similar polymers to compare the polymers' biodistribution [10] and found that the polymers accumulated at solid tumors in a "molecular-weight"-dependent manner. This molecular-weight dependency indicated that smaller molecular weights of polymers can be excreted through the kidneys.

These above-mentioned polymers exhibited better tumor accumulation, corresponded to larger molecular weights of the polymers. However, the excretion of the contrast agent, especially in the case of the macromolecular contrast agent, is a serious matter for the development of diagnostic agents.

Therefore, we checked the kidneys' excretion of our polymeric micelle contrast agent. In urine, 20.8±7.6% of the polymeric micelle was found 48 h after the injection. This result indicates that the polymeric micelle was excreted through the kidney filtration. Since the size of the polymeric micelle contrast agent was 50–250 nm as shown in Fig. 3(a), the polymeric micelles cannot pass through the kidney filtration. Therefore, these polymers that formed in urine appears to have passed through the kidney filtration in a dissociated polymer form, since the average molecular weight of this block copolymer is only 15,000. This is an excellent property of the polymeric micelle MRI contrast agent; namely, this agent exhibits long circulation in blood in a micelle form, while this agent can be excreted through the kidneys in a dissociated polymer form.

Furthermore, the obtained polymeric micelle MRI contrast agent delivered a larger amount to solid tumors than did previously reported macromolecular MRI contrast agents that can be also excreted from the kidneys (agents such as PHPMA gadolinium-conjugate [14] and graft copolymer of poly(ethylene glycol) with poly (L-lysine) [10]).

In order to estimate possible acute toxicity, we injected the 4-fold of the volume of the contrast agent into the mouse tail vein, and observed the body weight change over the course of 16 days. There was no significant difference in comparison to the control (less than ±10%). Although we have to conduct further experiments to obtain toxicity-related information of greater exactness, these preliminary results indicate that this polymeric micelle can dissociate and be excreted from the kidneys, and that this tumor targeting results a passive targeting mechanism (the EPR effect). In a future study, we would like to optimize the pharmacokinetics and the dissociation behavior of the polymeric micelles by controlling the composition of the block copolymers.

### 3.4. MR imaging at tumor tissue

We took an MR image of the tumor-bearing mouse after the injection of the polymeric micelle contrast agent. Fig. 6 shows $T_1$-weighted MR images of tumor tissues before and after 24 h at an injection dose of 0.05 mmol Gd/kg. After the injection of the polymeric micelle, MR images exhibited a significant signal enhancement at the kidneys. This signal enhancement at the kidneys indicates that kidneys excreted the contrast agent, as shown in Fig. 6(c). However, even 24 h after the injection, an intense signal was observed in the heart and aorta areas. This indicates that a considerable amount of the contrast agent was circulating in the bloodstream, as described in pharmacokinetic results. The relative signal intensity at axial slices of the tumor tissues underwent a 2.0-fold increase after 24 h, as compared with the signal before the injection. The signal intensity of the tumor area had gradually increased by 24 h and had slightly decreased by 48 h, as shown in Fig. 7. This behavior of the signal intensities is similar to the doxorubicin concentration delivered by the polymeric micelle carrier system. All these results indicate that the enhancement of MR signals in the tumor area rested on the successful passive accumulation of the MRI contrast agent at solid tumors.

## 4. Conclusion

We prepared polymeric micelle MRI contrast agents using poly (ethylene glycol)-*b*-poly(L-lysine) block copolymers. A reaction of poly(ethylene glycol)-*b*-poly(L-lysine) with a DOTA derivative resulted in a quantitative DOTA conjugation regarding the lysine residues of the block copolymer, and the obtained block copolymer formed a polymeric micelle. This micellar structure was maintained after a partial chelation of the DOTA moiety with gadolinium ions. The biodistribution and the excretion of the polymeric micelle was evaluated in colon 26-bearing $CDF_1$ female mice. Selective accumulation of the polymeric micelle at the tumor tissues was observed 24 h after the injection. The contrast agent's accumulation substantially enhanced the signal intensity of the MR images at the tumor. This polymeric micelle MRI contrast agent will be a useful diagnostic tool, particularly in combination with a polymeric micelle-based drug-targeting system.

## Acknowledgement

This work was supported by the Ministry of Health, Labour, and Welfare of Japan. K. Shiraishi and M. Yokoyama acknowledge the support from the Program for Promoting the Establishment of Strategic Research Centers, Special Coordination Funds for Promoting Science and Technology, the Ministry of Education, Culture, Sports, Science and Technology of Japan, and Tokyo Ohka Foundation for the Promotion of Science and Technology.

## Appendix A. Supplementary data

Supplementary data associated with this article can be found, in the online version, at doi:10.1016/j.jconrel.2009.01.010.

## References

[1] M. Yokoyama, T. Okano, Y. Sakurai, S. Fukushima, K. Okamoto, K. Kataoka, Selective delivery of adriamycin to a solid tumor using a polymeric micelle carrier system, J. Drug Target. 7 (3) (1999) 171–186.

Please cite this article as: K. Shiraishi, et al., Preparation and in vivo imaging of PEG-poly(L-lysine)-based polymeric micelle MRI contrast agents, J. Control. Release (2009), doi:10.1016/j.jconrel.2009.01.010

[2] Y. Matsumura, H. Maeda, A new concept for macromolecular therapeutics in cancer chemotherapy: mechanism of tumoritropic accumulation of proteins and the antitumor agent Smancs, Cancer Res. 46 (1986) 6387–6392.
[3] H.M. Aliabadi, A. Lavasanifar, Polymeric micelles for drug delivery, Expert Opin. Drug Deliv. 3 (1) (2006) 130–162.
[4] N. Nishiyama, S. Okazaki, H. Cabral, M. Miyamoto, Y. Kato, Y. Sugiyama, K. Nishio, Y. Matsumura, K. Kataoka, Novel cisplatin-incorporated polymeric micelles can eradicate solid tumors in mice, Cancer Res. 63 (2003) 8977–8983.
[5] N. Nishiyama, M. Yokoyama, T. Aoyagi, T. Okano, Y. Sakurai, K. Kataoka, Preparation and characterization of self-assembled polymer–metal complex micelle from cis-dichlorodiammineplatinum(II) and poly(ethylene glycol)-poly(α,β-aspartic acid) block copolymer in an aqueous medium, Langmuir 15 (1999) 377–383.
[6] A. Bogdanov Jr, C. Martin, A.V. Bogdanova, T.J. Brady, R. Weissleder, An adduct of cis-diamminedichloroplatinum(II) and poly(ethylene glycol)poly(L-lysine)-succinate: synthesis and cytotoxic properties, Bioconjug. Chem. 7 (1) (1996) 144–149.
[7] R. Rebizak, M. Schaefer, E. Dellacherie, Polymeric conjugates of $Gd^{3+}$-diethylenetriaminepentaacetic acid and dextran. 1. Synthesis, characterization, and paramagnetic properties, Bioconjug. Chem. 8 (4) (1997) 605–610.
[8] M.M. Huber, A.B. Staubli, K. Kustedjo, M.H.B. Gray, J. Shih, S.E. Fraser, R.E. Jacobs, T.J. Meade, Fluorescently detectable magnetic resonance imaging agents, Bioconjug. Chem. 9 (2) (1998) 242–249.
[9] A. Bogdanov Jr, S.C. Wright, E.M. Marecos, A.V. Bogdanova, C. Martin, R. Weissleder, A long-circulating co-polymer in "passive targeting" to solid tumors, J. Drug Target. 4 (5) (1997) 321–330.
[10] R. Weissleder, A. Bogdanov Jr, C-H. Tung, H-J. Weinmann, Size optimization of synthetic graft copolymers for in vivo angiogenesis imaging, Bioconjug. Chem. 12 (2) (2001) 213–219.
[11] F. Ye, T. Ke, E-K. Jeong, X. Wang, Y. Sun, M. Johnson, Z-R. Lu, Noninvasive visualization of in vivo drug delivery of poly(L-glutamic acid) using contrast-enhanced MRI, Mol. Pharm. 3 (5) (2006) 507–515.
[12] X. Wen, E.F. Jackson, R.E. Price, E.E. Kim, Q. Wu, S. Wallace, C. Charnsangavej, J.G. Gelovani, C. Li, Synthesis and characterization of poly(L-glutamic acid) gadolinium chelate: a new biodegradable MRI contrast agent, Bioconjug. Chem. 15 (6) (2004) 1408–1415.
[13] Z-R. Lu, X. Wang, D.L. Parker, K.C. Goodrich, H.R. Buswell, Poly(L-glutamic acid) Gd (III)–DOTA conjugate with a degradable spacer for magnetic resonance imaging, Bioconjug. Chem. 14 (4) (2003) 715–719.
[14] Y. Wang, F. Ye, E-K. Jeong, Y. Sun, D.L. Parker, Z-R. Lu, Noninvasive visualization of pharmacokinetics, biodistribution, and tumor targeting of poly[N-(2-hydroxypropyl)methacrylamide] in mice using contrast enhanced MRI, Pharm. Res. 24 (6) (2007) 1208–1216.
[15] H. Kobayashi, M.W. Brechbiel, Dendrimer-based macromolecular MRI contrast agents: characterization and application, Mol. Imag. 2 (1) (2003) 1–10.
[16] H. Kobayashi, S. Kawamoto, S-K. Jo, H.L. Bryant Jr, M.W. Brechbiel, R.A. Star, Macromolecular MRI contrast agents with small dendrimers: pharmacokinetic differences between sizes and cores, Bioconjug. Chem. 14 (2) (2003) 388–394.
[17] H. Kobayashi, N. Sato, S. Kawamoto, T. Saga, A. Hiraga, T.L. Haque, T. Ishimori, J. Konishi, K. Togashi, M.W. Brechbiel, Comparison of the macromolecular MR contrast agents with ethylenediamine-core versus ammonia-core generation-6 polyamidoamine dendrimer, Bioconjug. Chem. 12 (1) (2001) 100–107.
[18] E. Nakamura, K. Makino, T. Okano, T. Yamamoto, M. Yokoyama, A polymeric micelle MRI contrast agent with changeable relaxivity, J. Control. Release 114 (2006) 325–333.
[19] V.P. Torchilin, PEG-based micelles as carriers of contrast agents for different imaging modality, Adv. Drug Deliv. Rev. 54 (2002) 235–252.
[20] G. Zhang, R. Zhang, X. Wen, L. Li, C. Li, Micelles based on biodegradable poly(L-glutamic acid)-b-polylactide with paramagnetic Gd ions chelated to the shell layer as a potential nanoscale MRI-visible delivery, Biomacromolecules 9 (1) (2008) 36–42.
[21] H.Y. Lee, H.W. Jee, S.M. Seo, B.K. Kwak, G. Khang, S.H. Cho, Diethylenetriamine-pentaacetic acid–gadolinium (DTPA–Gd)-conjugated polysuccinimide derivatives as magnetic resonance imaging contrast agents, Bioconjug. Chem. 17 (3) (2006) 700–706.
[22] N. Nasongkla, E. Bey, J. Ren, H. Ai, C. Khemtong, J.S. Guthi, S-F. Chin, A.D. Sherry, D.A. Boothman, J. Gao, Multifunctional polymeric micelles as cancer-targeted, MRI-ultrasensitive drug delivery systems, Nano Lett. 6 (11) (2006) 2427–2430.
[23] Z-R. Lu, F. Ye, A. Vaidya, Polymer platforms for drug delivery and biomedical imaging, J. Control. Release 122 (2007) 269–277.
[24] M. Yokoyama, G.S. Kwon, T. Okano, Y. Sakurai, M. Naito, K. Kataoka, Influencing factors on in vitro micelle stability of adriamycin-block copolymer conjugate, J. Control. Release 28 (1994) 59–65.
[25] Y. Takakura, T. Fujita, M. Hashida, H. Sezaki, Disposition character of macromolecules in tumor-bearing mice, Pharm. Res. 7 (4) (1990) 330–346.
[26] A. Harada, K. Kataoka, Formation of polyion complex micelles in an aqueous milieu from a pair of oppositely-charged block copolymers with poly(ethylene glycol) segments, Macromolecules 28 (15) (1995) 5294–5299.

Please cite this article as: K. Shiraishi, et al., Preparation and in vivo imaging of PEG-poly(L-lysine)-based polymeric micelle MRI contrast agents, J. Control. Release (2009), doi:10.1016/j.jconrel.2009.01.010